smaller in magnitude, as low as $-0.20a_0^3$ mm/sec. Ingalls[30] has given an analysis for Fe^{57} in iron which takes into account both scaling in the 4s part of the conduction band and $s \rightarrow d$ (or $d \rightarrow s$) transfer of electrons in the 4s-3d band, changing the shielding of the 3s electrons. His results can be put in the form[26]

$$d(M\epsilon)/d\ln V = \alpha[-4.86+12.05X], \qquad (14)$$

where $X = dN_s/d\ln V$ is the change in number of 4s electrons with fractional volume change in the 4s-3d band. This is assumed in first order to be equal to $-\partial N_d/\partial \ln V$.

It is not obvious that this relationship should apply to Fe^{57} in dilute solution in other metals. We shall here assume that it does. For Fe^{57} dissolved in a number of first-row transition metals the isomer shifts cluster around that for metallic iron in a band quite narrow compared, say, with the difference between ferrous and ferric ion isomer shifts, giving a sort of zeroth-order validity to this assumption. In Fig. 9 are the plots of α versus X including our recently published data for iron. The grouping of close-packed and bcc systems is obvious. For iron, Stern's[31] calculations indicate a positive value for X. In any case, it is quite clear that if there is no $s \leftrightarrow d$ transfer in one structure, it must occur in the other, and that, in general, the close-packed systems have a greater tendency for s-to-d electron transfer.

[30] R. Ingalls, Phys. Rev. **155**, 157 (1967).

[31] F. Stern, Ph.D. thesis, Princeton University (unpublished).

PHYSICAL REVIEW VOLUME 172, NUMBER 3 15 AUGUST 1968

Reflectance and $1/\varepsilon$ Resonance of Beryllium in the Far Ultraviolet

J. TOOTS, H. A. FOWLER, AND L. MARTON
National Bureau of Standards, Washington, D. C. 20234

(Received 25 March 1968)

The reflectance of evaporated Be layers has been measured after 3-min exposure to ambient pressures of $\leq 3\times10^{-7}$ Torr, for the wavelength range of 480–1200 Å, for a spread of angles between 20° and 80°. These values give n and k by calculation; also, from these ϵ_1, ϵ_2, $\mathrm{Re}(1/\epsilon)$, and $\mathrm{Im}(1/\epsilon)$. The last two functions show good agreement with an inverted Drude-Sellmeier resonance formula. The center frequency of the resonance falls at 18.4±0.1 eV, corresponding to the natural plasma-resonance frequency of a free-electron gas with 2.0 electrons per atom; this confirms a 1948 prediction by A. Bohr. The half-width of the resonance is measured as 4.7±0.1 eV; this value is also obtained, within ±10%, from a sum-rule approximation, and is thought to represent an upper limit of the systematic error. This value corresponds to a decay time (for intensity) of the plasma oscillation of about 1.3×10^{-16} sec. An Argand-diagram display of the data is given, and the "longitudinal" Kramers-Kronig relationship is demonstrated.

I. INTRODUCTION

NUMEROUS studies of the "plasmon" dielectric excitation in solids by fast-electron energy losses[1–8] have shown the collective, or many-electron, nature of this phenomenon. In a 1948 paper on proton stopping, Bohr[9] proposed that beryllium should exhibit a simple form of this "longitudinal" dielectric resonance, in which two conduction electrons per atom would form an ideal free-electron gas resonating at 18 eV.

The present measurement appears to confirm Bohr's prediction in considerable detail. The electron-gas resonance, whose center turns out to lie at 18.4 eV (corresponding to the integral number 2 electrons per atom, within ±2%, when all errors of the comparison are considered), may be accurately fitted with an inversion of the semiclassical Drude-Sellmeier functions in a manner previously suggested by Fano[10,11] and by LaVilla and Mendlowitz.[12]

These measurements show a significant improvement over previous[12] Be optical data in the far ultraviolet. Measurement of reflectances at a number of incident angles permits the optical constants to be determined independently at each wavelength. The full spectral range of the free-electron-gas resonance is covered. The vacuum conditions have been improved, so that surface-contamination effects have been greatly reduced.

[1] L. Marton, J. Arol Simpson, H. A. Fowler, and N. Swanson, Phys. Rev. **126**, 182 (1962).
[2] H. Raether, Ergeb. Exakt. Naturw. **38**, 84 (1965).
[3] J. Hubbard, Proc. Phys. Soc. (London) **A68**, 976 (1955).
[4] H. Frohlich and H. Pelzer, Proc. Phys. Soc. (London) **A68**, 525 (1955); P. Nozières and D. Pines, Phys. Rev. **109**, 762 (1958); D. Bohm and D. Pines, *ibid.* **92**, 609 (1953); D. Pines, *ibid.* **92**, 626 (1953).
[5] L. Marton, L. B. Leder, and H. Mendlowitz, Advan. Electron. Electron Phys. **7**, 183 (1955), especially pp. 225 ff.
[6] N. Swanson, J. Opt. Soc. Am. **54**, 1130 (1964).
[7] R. H. Ritchie, Phys. Rev. **106**, 874 (1957).
[8] N. Swanson and C. J. Powell, Phys. Rev. **145**, 195 (1966).
[9] A. Bohr, Kgl. Danske Videnskab. Selskab, Mat.-Fys. Medd. **14**, 19 (1948).
[10] U. Fano, Phys. Rev. **103**, 1202 (1956).
[11] U. Fano, Ann. Rev. Nucl. Sci. **13**, 1 (1963), especially pp. 17–19.
[12] R. E. LaVilla and H. Mendlowitz, Appl. Opt. **4**, 955 (1965).

II. EXPERIMENTAL METHOD

A description of the reflectometer and method of taking data can be found elsewhere.[13,14] The important aspects are as follows:

Ultraviolet radiation is produced by argon or nitrogen discharge in a duoplasmatron,[15] and the wavelength is selected by a platinum-coated normal-incidence grating. Polarization introduced by the grating has not been measured, but is thought to be small, since the tilt angles do not exceed 2°.

Optimum ambient pressure in the measurement chamber is 1×10^{-7} Torr and rises to 3×10^{-7} Torr when the duoplasmatron is in operation. A gettering-ion pump is used to reduce the partial pressure of the active gases.

Beryllium is evaporated from tantalum boats onto glass substrates situated 20 cm above the boat level. Evaporation speeds, estimated from flash duration and measurement of the film thicknesses, are about 50 A/sec. However, with no shutter available, the speeds are variable from one evaporation to another, and during an evaporation. Thickness of the total beryllium layer varies from 300 to greater than 1000 Å; the measurements reported below appear to be independent of whether the beryllium surface is backed by other layers of beryllium or by glass. However, when film thickness grows appreciably over 1000 Å, the reflectance drops. We suspect this to be a surface-roughening effect,[16] especially since the reflectances of angles near normal incidence are lower than would be expected from values at the higher incidence angles. Wide detector acceptance angle prevents us from an accurate determination of the scattering. Reflection electron diffraction at 80 keV (near grazing incidence), made after exposure to atmosphere, indicates these films to be polycrystalline Be, with four lattice spacings identifiable as those of the hexagonal close-packed structure.

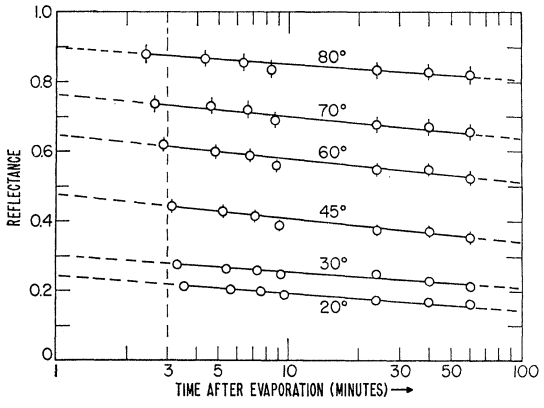

FIG. 1. Reflectance-history diagram of an evaporated Be film. Reflectance for six angles of incidence is shown for $\lambda=660$ Å as a function of time after the evaporation flash (semilog plot).

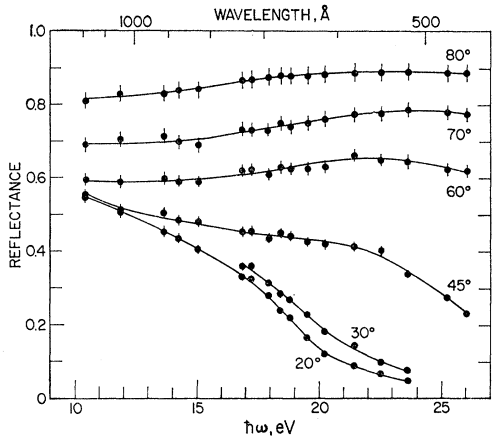

FIG. 2. 3-min reflectance as a function of wavelength for evaporated Be films. Experimental points are taken from a different specimen, or specimens, for each wavelength; they correspond to the common vertical dashed 3-min line in Fig. 1. Curves are smooth fits to the data points. Error bars indicate limits of measurement error in the individual points.

During the evaporation flash, which takes place in a sidearm, the gauge reading in the measurement chamber jumps to $(2\text{–}3)\times10^{-6}$ Torr and falls back to the ambient level within a few seconds after evaporation. The pressure rise in the evaporation sidearm is higher, but is not accurately known.

After evaporation, the specimen is transferred to the measurement chamber, where the first measurements can be made about 2 min after the evaporation flash. About 2 min are needed to measure the reflectances of six incident angles at one wavelength. The primary beam intensity is checked before and after measuring each set of reflected intensities.

Some of the data which emerge from these measurements are shown in Fig. 1. Reflectance at six angles of incidence is shown, for 660 Å (18.8 eV), as a function of time after the evaporation flash (shown logarithmically). Between 2 and 60 min after evaporation, the reflectance decline is a close approximation to exponential decay. We refer to such a plot as a "reflectance history"; the slopes of the plots are different for each wavelength.

Because of the reflectance decline with time, presumably caused by surface contamination, we have had to evaporate a fresh layer of Be for measurements at each wavelength. Reflectance values are shown as a function of wavelength in Fig. 2; these points indicate the reflectance-history values at the common 3-min mark indicated by the vertical dashed line in Fig. 1. All are based on data taken between 2 and 4 min after the evaporation flash. The error bars indicate the estimated probable error resulting from meter readings.

[13] L. Marton, J. A. Simpson, J. A. Suddeth, and L. B. Leder, in *Transactions of the Eighth Vacuum Symposium and Second International Congress*, edited by L. E. Preuss (Pergamon Press, Inc., New York, 1961), p. 633.
[14] L. Marton and J. Toots, Phys. Rev. **160**, 602 (1967).
[15] J. A. R. Samson and H. Liebl, Rev. Sci. Instr. **33**, 1340 (1962).
[16] L. S. Palatnik and A. I. Fedorenko, Fiz. Metal. i Metalloved. **18**, 69 (1964).

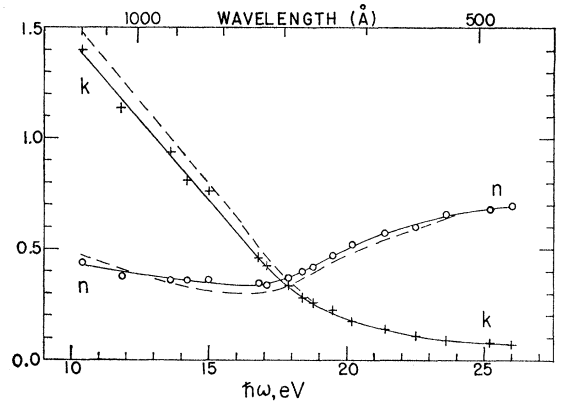

FIG. 3. n and k values calculated from the points of Fig. 2 by the Fresnel equations (Ref. 16), assuming zero polarization. The points are obtained from the extreme values of reflectance (20° and 80°, except from 23 to 26 eV, where 45° and 80° are used). Dashed curves: from reflectance-history lines extrapolated to 0.5 min.

Data taken at later times yielded points on the reflectance history of each specimen at a number of different wavelengths; these were used to check reproducibility from one specimen to the next. All data were rejected from specimens which did not follow the common reflectance histories, within $\pm 2\%$ of the incident beam intensity. Since the rejected data invariably exhibited lower reflectances, we feel that the reproducible high-reflectance data are our best approximation to characteristics of a clean beryllium surface.

III. COMPUTED OPTICAL CONSTANTS

The optical constants n and k can be calculated by Fresnel's[17] equations, if the reflectance values are known for at least two angles of incidence. Measurements at additional incidence angles provide a criterion for additional information about the self-consistency of the data. Figure 3 shows the values of n and k calculated from the extreme-angle points of Fig. 2 (20° and 80°, except from 23 to 26 eV, where 45° and 80° are used), assuming negligible polarization.

For photon energies over 21 eV our data display a high degree of self-consistency, but at lower energies we find a discrepancy that is quite systematic. The n and k values calculated from our reflectances at the extreme angles, which should be the most sensitive combination for determining n and k, require higher reflectances than those actually observed, for the intermediate angles. This effect is well outside the measurement error, and reproducible for different specimens.

Data taken with the same instrument on some other materials[14] exhibit no such inconsistency. Thus the effect does not appear to be the result of a particular systematic error introduced by the equipment (such as polarization). A more probable cause of this discrepancy may be inferred from a study of the reflectance histories. At longer wavelengths (photon energies below 21 eV) the reflectance history lines of the intermediate angles exhibit a steeper slope with time than those of the extreme angles. This effect is apparent, although not very drastic, in Fig. 2. Extrapolating backward in time[18] improves the internal consistency of the data by decreasing the deviation for a set of n and k values which solve the Fresnel equations for reflectance. Optimum internal consistency is reached when the reflectance values are extrapolated to 0.5-min mark on the reflectance-history curve. The n and k values calculated from these extrapolated reflectances are shown as broken lines in Fig. 3. However, the extrapolated values depend too heavily on conjecture and cannot be considered reliable values.

The fact that extrapolating backward in time to higher reflectances increases the apparent internal consistency of the data suggests that the reflectances at the extreme angles, where the change with time is slowest, represent our best measured values. Therefore the reflectances at the extreme angles, rather than a best fit to all the measured values at each wavelength, have been used in point-by-point calculation of n and k in Fig. 3 and the optical parameters calculated in subsequent figures.

The errors indicated by bars in Fig. 2 produce a spread in n and k values when propagated through the Fresnel equations. The problem is less severe on the high-energy side—above 19 eV—where the maximum spread is $\pm 5\%$ for n and $\pm 10\%$ for k; on the low-energy side of the spectrum the values range up to twice these magnitudes. The close local continuity of the n and k indicates that the actual random errors are smaller. We have considered the errors of the optical system as discussed by Hunter[18]; with the possible exception of a systematic error introduced by polarization, they appear to be less important than the uncertainties resulting from instrument reading. We feel, however, that the most serious limitation of these measurements is a systematic error resulting from the surface changes that occur prior to our first measurements.

Reflectance of the intermediate angles shown in Fig. 2 suggests a set of n and k values that deviate by a maximum of 15% from our points on Fig. 3. The greatest difference is a higher value of n near the n minimum, around 16 eV, while only small differences are noted at the higher energies. The reflectance decline as film ages increases the n values, while the change in k is less systematic and not always monotonic with time. Reflectances of the specimens which fell outside the reproducibility criterion and were rejected ranged from slightly to considerably lower values than those shown in Fig. 2. Internal consistency for Fresnel solutions in

[17] R. Tousey, J. Opt. Soc. Am. **29**, 235 (1939); I. Simon, *ibid.* **41**, 336 (1951); I. Sasaki and K. Ishiguro, Japan. J. Appl. Phys. **2**, 289 (1963); O. S. Heavens, Phys. Thin Films **2**, 727 (1964); W. R. Hunter, J. Opt. Soc. Am. **55**, 1197 (1965).

[18] W. R. Hunter, J. Appl. Opt. **6**, 2140 (1967).

these rejected specimens was generally poor. In some cases the n values, as calculated from the extreme-incident-angle reflectances, were 50% higher than those of the accepted data.

The previous optical data have been too fragmentary,[19–21] in addition to being taken under unsatisfactory vacuum conditions, to permit a meaningful comparison with our measurements. More to the point is a comparison with the optical properties deduced by LaVilla and Mendlowitz from electron-scattering data. Close agreement is found with the set of optical constants deduced from Swanson's[22] electron-scattering spectrum I, which is shown in Fig. 4. The n and k values are almost identical above 19 eV, maximum deviation occurring around 15 eV, where their n value is about 10% higher than ours.

The values of ϵ_1 and ϵ_2, the real and imaginary parts of the complex dielectric constant, are shown in Fig. 4 as they are calculated from the n and k points in Fig. 3. Also shown (as crosses, with a connecting continuous curve) is the function $-\mathrm{Im}(1/\epsilon)$, often referred to as the energy-loss function; it traces out the probability of characteristic energy losses[2,7,10] suffered by fast charged particles traversing the material. In this form our data can be compared with the electron-scattering spectrum of Swanson,[6,12] which is indicated by the broken line, normalized to our data at its peak. This (modified) electron-scattering spectrum[22] has a width at half-maximum of 5.1 eV. Since errors in both optical-reflectance and electron-scattering experiments tend to broaden the observed line shape, our data appear to represent an improved determination of the line form. The continuous curve connecting our experimental points calculated from our n and k fit in Fig. 3 displays a half-width of 4.5 eV. The maximum amplitude is found at 18.2 eV; the magnitude is 4.0 ± 0.1 (no comparable figure for amplitude is obtainable from the electron-scattering experiment).

IV. INTERPRETATION

The interpretation of these experimental curves is greatly facilitated by a further step of calculation from the Fresnel-equation values of n and k. We follow the suggestion made by Fermi[23] in 1940, that the inverse dielectric function $1/\epsilon$ best represents the "distributed" structure of a longitudinal electromagnetic resonance in a solid; we calculate both *real* and *imaginary* parts of this function from the relations

$$\mathrm{Re}(1/\epsilon)=(n^2-k^2)/(n^2+k^2)^2=\epsilon_1/(\epsilon_1^2+\epsilon_2^2), \quad (1)$$

$$\mathrm{Im}(1/\epsilon)=2nk/(n^2+k^2)^2=-\epsilon_2/(\epsilon_1^2+\epsilon_2^2). \quad (2)$$

[19] G. B. Sabine, Phys. Rev. **55**, 1064 (1939).
[20] M. Banning, J. Opt. Soc. Am. **32**, 98 (1942).
[21] S. Robin, J. Phys. Radium **14**, 427 (1953).
[22] See N. Swanson (Ref. 6). This curve is not based upon the raw data of Swanson; background has been eliminated by LaVilla and Mendlowitz (Ref. 12), who use this curve as spectrum No. 1 in deducing optical properties.
[23] E. Fermi, Phys. Rev. **57**, 485 (1940).

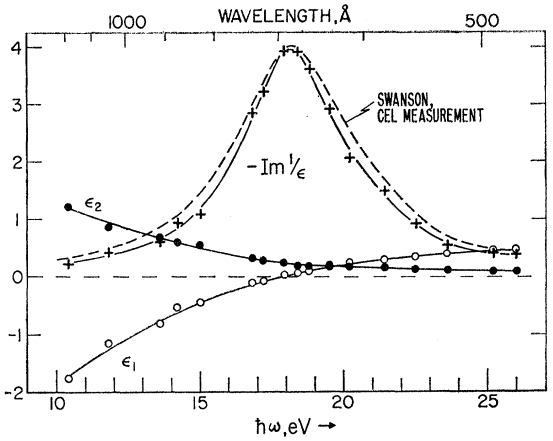

FIG. 4. Dielectric constants ϵ_1 and ϵ_2 calculated point-by-point from n and k values in Fig. 3. Crosses: $-\mathrm{Im}(1/\epsilon)$, connected by the smooth continuous curve (no analytic significance). Dashed curve: electron-scattering spectrum of Swanson (Ref. 6), as reduced by LaVilla and Mendlowitz (Ref. 12) (spectrum No. 1), normalized to the peak data points of our measurement.

Starting from the point-by-point values of Fig. 3, we obtain the circles and points shown in Fig. 5, for real and imaginary parts of $1/\epsilon$ as functions of frequency.

In the frequency dependence of the real, or "phase-dependent," part, the region of anomalous dispersion runs from negative to positive with increasing frequency —because we are dealing here with an inverse dielectric function. This reversed resonant form in the real part has not been previously demonstrated in the experimental literature. Although plots of $\mathrm{Re}(1/\epsilon)$ from previous experiments may show an offset at the longitudinal resonance, they do not resolve the clear minimum-and-maximum seen in these experimental points. In fact, our measurements, if evaluated at the point $t=10$ min in the reflectance-history curves, Fig. 1, no longer resolve this detail.

The smooth curves shown in Fig. 5 are calculated by taking the conventional Drude-Sellmeier formulas[7,10,12] and inverting the sign of the polarizability, thus:

$$\mathrm{Re}(1/\epsilon)=1-\frac{\omega_I^2[\omega_I^2-\omega^2]}{[\omega_I^2-\omega^2]^2+\omega_{II}^2\omega^2}, \quad (3)$$

$$\mathrm{Im}(1/\epsilon)=-\frac{\omega_I^2\omega_{II}\omega}{[\omega_I^2-\omega^2]^2+\omega_{II}^2\omega^2}. \quad (4)$$

These two parts of the inverse dielectric function are linked by an internal Kramers-Kronig relationship[24] similar to that between ϵ_1 and ϵ_2.[25–27]

[24] T. S. Moss, *Optical Properties of Semiconductors* (Butterworths Scientific Publications Ltd., London, 1959), Appendix B, p. 245. The proof given here is independent of the sign assumed for the polarizability.
[25] H. R. Philipp and E. A. Taft, Phys. Rev. **113**, 1002 (1959); **120**, 37 (1960); **127**, 159 (1962).
[26] H. Ehrenreich and H. R. Philipp, Phys. Rev. **128**, 1622 (1962); **129**, 1550 (1963).
[27] H. Ehrenreich, H. R. Philipp, and B. Segall, Phys. Rev. **132**, 1918 (1963).

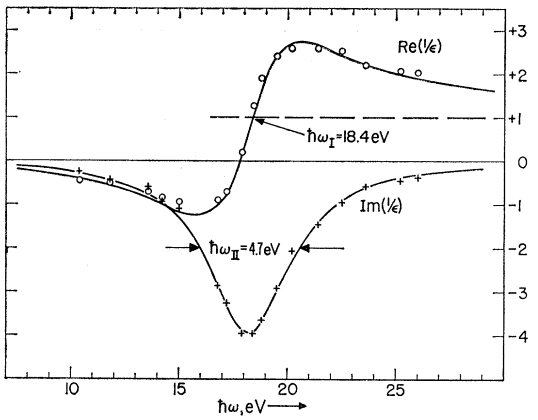

FIG. 5. Real and imaginary parts of $1/\epsilon$. Circles and points are calculated by Eqs. (1) and (2) from the n and k values of Fig. 3. Both parts are plotted with the same sign convention as is used for ϵ_1 and ϵ_2 in Fig. 4. Note that the region of anomalous dispersion runs from negative to positive with increasing frequency. Smooth curves are calculated by Eqs. (3) and (4), using the values of ω_I and ω_{II} given in Eqs. (5) and (6).

The form of the imaginary part has already been proposed by LaVilla and Mendlowitz[12]; what we have done here is to add the real part in the manner suggested by Fano[10] for the solutions of his secular equation. ω_I and ω_{II} are the *only* parameters of this model, determining amplitude as well as shape and position. They have been chosen in the following way:

$$\omega_I=\omega_p=(4\pi ne^2/m)^{1/2}=18.4\text{ eV}/\hbar, \qquad (5)$$

where e is the "bare" electronic charge, m is the free-electron mass, and n is taken to be the density 2.0 electrons per atom, using the x-ray atomic density of the hexagonal close-packed lattice.[28]

ω_{II}, the width at half-maximum of the imaginary part, represents the reciprocal decay time of the longitudinal oscillation. Fitting the two parts of the resonance across its entire width by a series of 0.1-eV/$\hbar$ variations in ω_{II}, with ω_I fixed at the above value, we find a best value

$$\omega_{II}=4.7\text{ eV}/\hbar, \qquad (6)$$

which corresponds to a lifetime (for intensity decay) of about 1.3×10^{-16} sec. Since Eqs. (3) and (4) resemble the form of a damped classical oscillator, the linewidth can also be estimated coarsely from the amplitude, by the relation $\omega_{II}=\omega_p/\max|\mathrm{Im}1/\epsilon|$, where $\max|\mathrm{Im}1/\epsilon|$ is the maximum value of the peak in Fig. 4.[29,30] This gives $\omega_{II}=4.6$ eV/$\hbar$.

The lifetime is very short by optical standards, corresponding to only a cycle or two in the visible frequency range. It is sufficiently long, however, with respect to a far-ultraviolet oscillation, to permit a well-defined resonance with a meaningful center frequency ω_I. Note that the resonance described by Eqs. (3) and (4) is a single, centered response of roughly symmetrical form.

The fit between theory and experiment is seen to be good. Such details as the slight asymmetry of $\mathrm{Re}(1/\epsilon)$ and its asymptotic limits are brought out in the comparison of Fig. 5. The small discrepancy remaining in $\mathrm{Re}(1/\epsilon)$ between theory and experiment, from 12 to 16 eV, can be satisfactorily explained by the slight surface contamination thought to be present. (Any effects of polarization in the incident radiation are also most likely to appear at these long wavelengths.)

The real part passes through zero very near 18 eV—in very close agreement with Bohr's prediction. It passes through the line (+1) at frequency $\omega_I=18.4\pm0.05$ eV/$\hbar$, the natural plasma-resonance frequency for 2.0 electrons per atom. The error-in-definition of this intersection is less than $\pm1\%$ of ω_I, and a perceptibly poorer fit to the resonance curves is obtained if ω_I is varied by as little as 0.1 eV/$\hbar$. This suggests that the electron gas is undergoing a "pure" semiclassical resonance, free of lattice binding.

The imaginary part has its largest amplitude at or near 18.2 eV, slightly below the value of 18.45 estimated by Swanson[12,22] in his electron-energy-loss experiment. As may be seen in Fig. 4, however, these two results are compatible, within the errors ascribable to the energy-loss experiment (from which primary energy-spread and plural-scattering background can never be completely eliminated). This largest amplitude is very nearly identical to the minimum-to-maximum swing of the real part.

The fit between theory and experiment is shown in a different manner in Fig. 6, which shows imaginary part of $1/\epsilon$ plotted against real part, with $\hbar\omega$ indicated along the curve as an implicit variable. The crosses are the experimental points, and the curve corresponds to a combined representation of Eqs. (3) and (4), with ω_I and ω_{II} fixed by (5) and (6). This yields a curve which is very nearly circular, except as it approaches zero frequency (note that experiment and theory agree at this end, to the limit of our spectral range). The center C is well defined from experiment, between 16 and 26 eV, and lies at $\mathrm{Re}1/\epsilon\cong0.75$, $\mathrm{Im}1/\epsilon\cong-2.0$.

The circle defined by the experimental points has its origin in a similar resonance circle which describes transverse ($\epsilon_1\epsilon_2$) resonances in the "visible" frequency region (see, for example, the circle shown for germanium by Moss[31]). Conformal inversion of ϵ through a unit circle [Eqs. (1) and (2)] reverses the sense of Moss's circle with increasing frequency and drops it from the top-half plane to the bottom half-plane. This algebraic

[28] H. H. Hausner, *Beryllium, Its Metallurgy and Properties* (University of California Press, Berkeley, 1965).

[29] In a more exact form suggested by the work of LaVilla and Mendlowitz (Ref. 12), this relation may be expressed as

$$\omega_{II}=\frac{\epsilon_1^2(\omega_m)+\epsilon_2^2(\omega_m)}{\epsilon_2(\omega_m)}\omega_p,$$

where $\epsilon_1(\omega_m)$ and $\epsilon_2(\omega_m)$ are evaluated (from Fig. 4, e.g.) at the frequency-for-maximum of the "stopping-power" function $\omega|\mathrm{Im}1/\epsilon|$. This "sum-rule linewidth" is a generalization of one due to Kanazawa (Ref. 30).

[30] H. Kanazawa, Progr. Theoret. Phys. (Tokyo) **26**, 851 (1961).

[31] T. S. Moss, Ref. 24, p. 19.

inversion (in going from a transverse to a longitudinal mode of dielectric oscillation) is responsible for the negative sign of the polarization in Eqs. (3) and (4) and for the "reversed" anomalous dispersion seen in Fig. 5.

On an $(\epsilon_1\epsilon_2)$ plot in the top half-plane, the points of Fig. 4 will cover only a small segment of arc (about 30°) around a center at $\epsilon_1 \cong +1.5$ and $\epsilon_2 \cong +4.2$. The major portion of the curve, describing transverse resonant excitations in the visible spectrum, lies beyond the low-frequency limit of our observations.

Our extension of the Drude-Sellmeier theoretical curve to zero frequency is an idealization which ignores the detailed structure of transverse resonances in the visible region. It is introduced only to show the mathematical consequences of Eqs. (3) and (4) at the low-frequency limit. Note that these equations *do not appear to be limited to small excursions* in frequency about ω_I, or in $\mathrm{Re}(1/\epsilon)$, about $+1$.

Since our data are limited to the far ultraviolet, we can make no statements about conduction-gas and band-edge effects in the "visible" spectrum. Both may contribute, in the manner suggested by Wilson.[32] The nearest band edge is thought, from optical data by Sabine[19] and Banning,[20] to terminate around 9 eV. X-ray-absorption-edge observations by Lukirskii and Brytov[33] place the major absorption structure between 2 and 9 eV. None of this data is fully satisfactory as a quantitative measure of dielectric oscillator strength, however.

Bohr's prediction was based on three details peculiar to beryllium: (1) the large proportion (2 to 2) of conduction to inner-shell electrons; (2) the large frequency separation between the nearest band edge and the free-electron-gas resonance frequency (thus on the low-frequency side the free-electron gas is not displaced or distorted by dielectric "dispersion" effects)[32,34]; and (3) the "open" ultraviolet frequency band reaching up to the nearest x-ray (KL) transition edge, which does not appear until above 108 eV [33,35] (hence the resonance is not affected by "inner-shell mixing").[36] The circular form, defined by the experimental points in Fig. 6, is wholly compatible with Bohr's picture of the free-electron gas, resonating in an undistorted, "unpulled" longitudinal mode. Its plasma-resonance frequency and oscillator strength correspond to an integral number of "free" electrons per atom. In these respects, beryllium may offer an unusual example of correspondence to a simple classical case, recalling the original successes of the Drude-Sellmeier formula[37] in its application to the "transverse" anomalous dispersion of gases, liquids, and solids.[38]

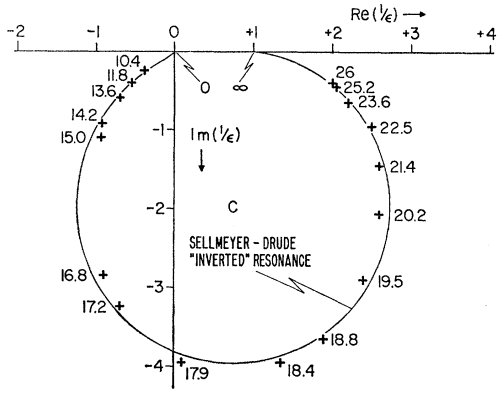

FIG. 6. Argand diagram of $1/\epsilon$. Crosses are the experimental values shown as circles and points in Fig. 5. Smooth curve: analytic solution to Eqs. (3)–(6). The points indicated as 0 and ∞ are the expected limits of this solution at $\omega=0$ and $\omega=\infty$. Frequencies, in eV/$\hbar$, are indicated for the experimental points. Point C, the experimentally defined center, is the locus of a singularity corresponding to the exponential-decay mode of the plasma oscillation.

The coincidence of ω_I with ω_p, the plasma frequency for a free-electron gas of density 2.0 electrons/atom, is as close as may be expected from the x-ray crystalline density,[39] which includes no consideration of dislocations, vacancies, or grain boundaries in the crystalline structure. The comparison, including the error of $\pm 1\%$ in determination of ω_I by curve fitting and a hypothetical error limit of $\pm 1\%$ in applying the x-ray density, appears to indicate agreement within $\pm 2\%$ to the resonance frequency of a semiclassical plasma. This agreement is more precise than would be expected from solid-state models of the conduction-electron gas,[37,38] particularly in view of the complicated Fermi surface of beryllium[40] and its positive Hall coefficient.[41]

The simplicity of this trial fit supports the quasi-classical free-electron-gas model of the longitudinal resonance, long advocated for stopping-power calculations by Lindhard[42] and generalized for a quantum-mechanical solid by Fano.[10,11,43]

[32] C. B. Wilson, Proc. Phys. Soc. (London) **76**, 481 (1960).

[33] A. P. Lukirskii and I. A. Brytov, Fiz. Tverd. Tela **6**, 43 (1964) [English transl.: Soviet Phys.—Solid State **6**, 33 (1964)].

[34] F. Stern, Progr. Solid State Phys. **15**, 299 (1963).

[35] J. A. Bearden, Rev. Mod. Phys. **19**, 1, 78 (1967), especially p. 86.

[36] M. W. Williams and E. T. Arakawa, J. Appl. Phys. **38**, 5272 (1967).

[37] P. Drude, *Theory of Optics* (Longmans, Green, and Co., London, 1902), especially pp. 394 ff.; Ann. Phys. **39**, 481 (1890), especially pp. 531 ff.; **64**, 159 (1898); see also J. C. Slater, *Quantum Theory of Molecules and Solids* (McGraw-Hill Book Co., New York, 1967), Vol. 3, pp. 3 ff.

[38] L. G. Schulz, Advan. Phys. **6**, 102 (1957).

[39] The plasma resonance frequency is most easily evaluated through the formula given by Kleinn (Ref. 50): $\hbar\omega_p = 28.8(z\sigma/A)^{1/2}$, where z is the assumed number of plasma electrons per atom, σ is the x-ray density, and A is the atomic weight. We employ the density 1.85 g/cc (Ref. 39), the x-ray value for the hcp lattice; the atomic weight of Be is 9.012 in the 1961 C^{12} system; see *Handbook of Chemistry and Physics* (Chemical Rubber Co., Cleveland, Ohio, 1964).

[40] T. L. Loucks and P. H. Cutler, Phys. Rev. **133**, A819 (1964); see also C. Herring and A. G. Hill, *ibid.* **58**, 132 (1940).

[41] F. Seitz, *The Modern Theory of Solids* (McGraw-Hill Book Co., New York, 1940), especially p. 183. The positive Hall coefficient, observed for beryllium, indicates that charge carriers in the conduction-electron gas undergo strong band interaction with the lattice.

[42] J. Lindhard, Kgl. Danske Videnskab. Selskab, Mat.-Fys. Medd. **28**, 8 (1954).

[43] U. Fano, NAS-NRC Publication 752 (Nuclear Science Series, Report No. 29), p. 158 ff. (unpublished).

The Argand diagram of Fig. 6 may also be pictured as a conformal (bilinear) mapping from the $(\omega'+i\omega'')$ complex-frequency plane, in which Eqs. (3) and (4) are a solution having four poles at $\pm\omega_{III}\pm\frac{1}{2}i\omega_{II}$, where $\omega_{III}=(\omega_I^2-\frac{1}{4}\omega_{II}^2)^{1/2}$. In Fig. 6, C is the mapped singularity representing *simple exponential decay* of the excited state. (The other three poles must also be considered in constructing a longitudinal "pulse" of finite duration, as in Coulomb excitation by fast charged particles, or in treating the phase and group velocities of the longitudinal waves in the plasma.)

The measurement of ω_{II} is more sensitive than ω_I to errors of the experiment. The observed linewidth, 4.7 $\pm$0.1 eV, is narrower than that previously reported from energy-loss experiment.[6] The direction of the remaining systematic error is such that the "true" linewidth may prove to be narrower yet; the extrapolated values of Fig. 3 would give a linewidth of 4.1 eV, with negligible shift in ω_I. This is taken as a measure of the possible remaining systematic error: The value 4.7 eV may be too large by about 12%.

Equations (3) and (4) do not specify a mechanism for the rapid decay of the excited "plasmon" state, which gives rise to the broad observed linewidth. The known existence of strong interband single-particle transitions at lower frequencies strongly suggests a decay channel into these transitions.

In this connection we may mention the conjecture of Pines[44] that a *Landau damping* of the longitudinal plasma waves (involving a close relation between the phase velocity of these waves and the velocity of electrons near the Fermi surface of the metals)[45–48] is responsible for the limiting decay process. Unfortunately, the existing experimental evidence on the strength of band-edge transitions[19–21,33] in beryllium does not permit an accurate evaluation of Pines's Landau-damping formula at the present time.

The mechanism of "many-particle" decay (more closely analogous to "collisional" plasma damping) has also been proposed, by Ninham, Powell, and Swanson[49]; it is thought to be pertinent near the cutoff of the electron-energy-loss experiment.[50–54]

V. CONCLUSIONS

From this detailed comparison of experiment with theory we are led to the following conclusions:

(a) Within the uncertainties remaining (from measurement errors and surface contamination), the measured real and imaginary parts of $1/\epsilon$ are in agreement with a simple ideal-electron-gas model, following Bohr's prediction.

(b) The center frequency ω_I, obtained by fitting the inverted Drude-Sellmeier resonance across the entire frequency spectrum from 10.4 to 26 eV, coincides to $\pm$1% with the "natural" plasma resonance frequency, 18.4 eV/$\hbar$, of a free-electron gas having 2.0 electrons per atom. The agreement is closer than could be expected from a solid-state model of a low-frequency conduction-electron gas, and is thought to represent a determination of this natural resonance frequency to better than $\pm$2% (allowing for error in applying the x-ray density).

(c) The Argand diagram suggests that the inverted Drude-Sellmeier resonance bears the expected relation to the optical constants ϵ_1 and ϵ_2 at lower frequencies and to the general secular equation for solid-state resonances suggested by Fano.[10]

(d) The linewidth ω_{II} is determined by curve fitting and by approximate sum rule to be 4.7$\pm$0.1 eV, the errors being those due to variational curve fitting and the random error in the experimental points. This is thought to represent an upper limit. Possible systematic error, associated primarily with the surface condition of the reflecting specimens, might be expected to render this value too high, by about 12% of the reported value. It corresponds to a lifetime for intensity decay of 1.3×10^{-16} sec.

(e) Plots of frequency dependence and Argand diagram for $1/\epsilon$ provide a sensitive display of internal data consistency in this far-ultraviolet-reflectance experiment. The resonance details of $\mathrm{Re}(1/\epsilon)$, which have not been previously investigated, appear to agree with an inverted Drude-Sellmeier formula, within the known random and systematic errors of the experiment.

ACKNOWLEDGMENTS

The authors wish to thank the following National Bureau of Standards colleagues for advice and assistance: R. P. Madden, R. LaVilla, H. Mendlowitz, U. Fano, and C. Powell. Helpful suggestions have been received from Professor Werner Brandt of New York University and Langdon T. Crane of the National Science Foundation.

[44] D. Pines, *Elementary Excitations in Solids* (W. A. Benjamin, Inc., New York, 1963), esp. p. 181. Dr. Langdon T. Crane, of the National Science Foundation, has called our attention to the mechanism of Landau damping.

[45] J. H. Malmberg and C. B. Wharton, Phys. Rev. Letters **19**, 775 (1967).

[46] I. A. Akhiezer, R. V. Polovin, A. G. Sitenko, and K. N. Stepanov, *Collective Oscillations in a Plasma* (MIT Press, Cambridge, Mass., 1967), esp. pp. 14 ff.

[47] J. G. Linhart, *Plasma Physics* (Amsterdam 1960), esp. pp. 102 ff.

[48] F. C. Shure, Ph.D. thesis, University of Michigan, 1963 (unpublished).

[49] B. W. Ninham, C. J. Powell, and N. Swanson, Phys. Rev. **145**, 209 (1966).

[50] W. Kleinn, Optik **11**, 226 (1954).

[51] H. Watanabe, J. Phys. Soc. Japan **11**, 112 (1956); **16**, 912 (1961).

[52] A. J. Glick and R. A. Ferrell, Ann. Phys. (N. Y.) **11**, 359 (1960).

[53] C. Kunz, Z. Physik **167**, 53 (1962).

[54] O. Sueoka, J. Phys. Soc. Japan **20**, 2203 (1965).